JOC The Journal of Organic Chemistry

Article

pubs.acs.org/joc

Asymmetric Michael Additions of 4-Hydroxycoumarin to β-Nitrostyrenes with Chiral, Bifunctional Hydrogen-Bonding Catalysts

Florian F. Wolf, Helge Klare, and Bernd Goldfuss*

Institut für Organische Chemie, Universität zu Köln, Greinstrasse 4, 50939 Köln, Germany

Supporting Information

ABSTRACT: Enantioselective Michael additions of 4-hydroxycoumarin to β-nitrostyrenes are catalyzed by different chiral, bifunctional hydrogen-bonding catalysts, based on thiourea- and squaramide motifs. The scope of the catalysis is tested by employing a series of substituted β-nitrostyrenes as well as different solvents. The 3,5-bis(trifluoromethyl)phenyl- and quinine-substituted squaramide catalyst is shown to be the most selective catalyst, resulting in 78% yield and 81% ee. Computational analyses of transition structures with different binding modes show that the most favored transition structure exhibits squaramide $(NH)_2$ binding to an oxygen atom of the enolate nucleophile, while the nitroalkene coordinates via hydrogen bonding to the ammonium function of the quinuclidine unit of the catalyst. Hence, the canted directionality of the squaramide $(NH)_2$ motif, favoring one-atom binding, might be decisive for the selectivity of the reaction. The absolute configuration of the major (−)-(*R*) enantiomer of the product is assigned computationally according to its optical rotation.

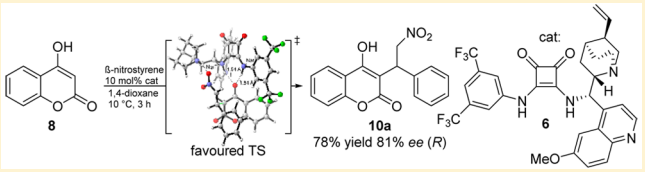

INTRODUCTION

Hydrogen-bonding (HB) catalysis has emerged as a major tool in organocatalytic applications.[1−5] (Thio-)urea-derived catalysts have proved to be highly efficient in many different reactions due to their high selectivity and yields.[6−12] Squaramide-based catalysts have been developed more recently as alternative hydrogen-bonding scaffolds.[13−16] The different and often superior performance of squaramide- vs (thio)urea-based catalysts[17−21] can be explained by altered hydrogen-bonding N−H alignments: in squaramides, these H−H distances are ca. 2.72 Å, in comparison to ca. 2.13 Å for thioureas.[17−19] Squaramides also show increased NH acidities of pK_a = 0.13−1.97 relative to thioureas,[20,21] supporting potentially stronger hydrogen bonds.[20,21] The directionality of NH hydrogen bonds may, however, dominate the catalyst−substrate interaction more than the relative acidities,[20,21] as is evident from comparative anion-receptor studies.[22−24] Squaramides show more canted NH groups in comparison to the nearly collinear alignment of the NH groups in (thio)ureas.[13−16]

Enantioselective Michael additions of 1,3-dicarbonyl compounds to β-nitroalkenes provide efficient pathways to γ-nitro carbonyl enantiomers, which can be used for further derivatizations.[25,26] 4-Hydroxycoumarin is an especially remarkable nucleophile for such enantioselective Michael additions, as the resulting 3-substituted 4-hydroxycoumarins are known to inhibit the enzyme vitamin K epoxide reductase, preventing the normal metabolic vitamin K formation.[27] The vitamin K antagonist warfarin serves as a most frequently employed anticoagulant and is also a rodenticide,[28−33] similar to other 3-substituted 4-hydroxycoumarins such as phenprocoumon[34] and acenocoumarol.[34] While chiral bifunctional thiourea catalysts were employed in Michael additions for the synthesis of 3-substituted 4-hydroxycoumarins,[6−16] only an achiral protocol for the addition of 4-hydroxycoumarin **8** to β-nitrostyrene **9** with reaction conditions "on-water" is available, providing 3-substituted 4-hydroxycoumarins **10** as racemates.[25] Although the tandem Michael addition/cyclization of β-nitrostyrene and 4-hydroxycoumarin catalyzed by chiral, bifunctional thioureas is known, resulting in an oxime product,[35] no squaramide-catalyzed reaction of those compounds has been reported so far.

Recently, we developed alkali-metal-mediated amino catalyses for enantioselective syntheses of 4-hydroxycoumarins with various Michael systems.[36] We also designed new cyclodiphosphazanes as hydrogen-bonding catalysts for enantioselective Michael additions of 4-naphthoquinone to β-nitroalkenes.[37]

In this work, we describe the scope of applications for chiral thiourea- and squaramide-hydrogen-bonding catalysts, based on enantiopure chinchona (**1**,[9] **2**, **3**,[10] **5**, **6**,[15] **7**[16]) and diaminocyclohexane (**4**[11]) units, in enantioselective Michael additions of 4-hydroxycoumarin to various β-nitroalkenes, yielding 3-substituted 4-hydroxycoumarins.

RESULTS AND DISCUSSION

Hydrogen-bonding catalysts with the established thiourea (**1**,[9] **2**, **3**,[10] **4**;[11] Figure 1) and squaramide units (**5**, **6**,[15] **7**;[16] Figure 2) have been employed in the Michael addition of 4-hydroxycoumarin **8** to β-nitrostyrene **9a** (Figure 3). Among the tested thiourea catalysts (**1**,[9] **2**, **3**,[10] **4**;[11] Figure 1), catalyst **3**[10] was most

Received: October 16, 2015
Published: January 27, 2016

DOI: 10.1021/acs.joc.5b02167
J. Org. Chem. 2016, 81, 1762−1768

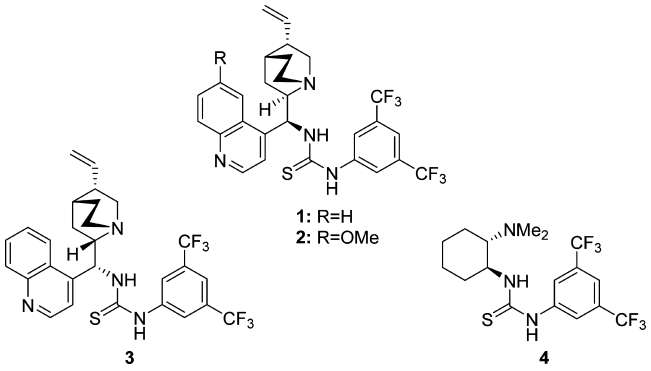

Figure 1. Thiourea-based hydrogen-bonding catalysts (**1**,[9] **2**, **3**,[10] **4**[11]) employed in this study.

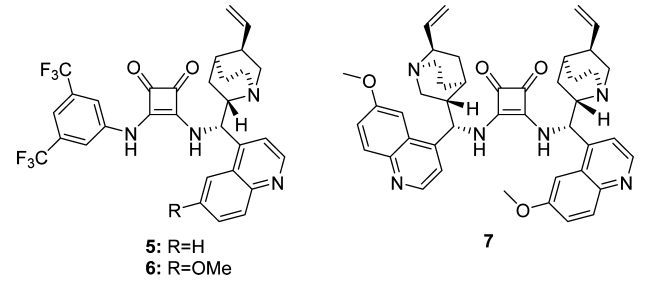

Figure 2. Squaramide-based hydrogen-bonding catalysts (**5**, **6**,[15] **7**[16]) employed in this study.

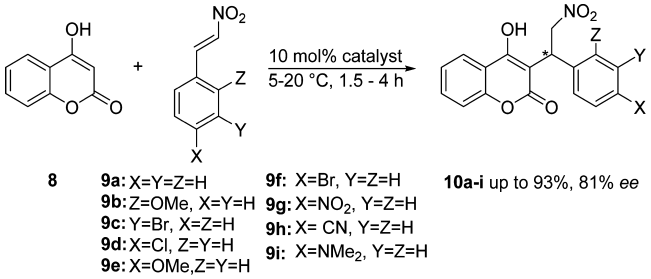

Figure 3. Michael addition of 4-hydroxycoumarin **8** to *β*-nitrostyrenes **9**, providing 3-substituted 4-hydroxycoumarins **10** (Tables 2 and 3).

reactive (64% yield; Table 1), while catalyst **2**[10] was the most selective (66% ee; Table 1). Among the tested squaramide catalysts (**5**, **6**,[15] **7**;[16] Figure 2), **6**[15] proved to be the most reactive and highly selective (92% yield, 72% ee; Table 1), while catalyst **5**[15] is slightly less reactive but is the most selective (80% yield, 74% ee; Table 1).

Hence, relative to the tested thiourea catalysts, the squaramide catalysts (Figure 2) provide increased reactivities, with lower reaction times and also higher enantioselectivities (Table 1). This superior catalytic performance of the squaramide systems agrees with a previous study,[24,37] emphasizing its strong hydrogen-bonding ability to nitrobenzene, in comaprison to urea, thiourea, phosphorus triamides, and cyclodiphosphazanes.

The high catalytic activity of the squaramide catalysts also parallels their higher NH acidities relative to thioureas.[38]

To optimize the reaction conditions in the enantioselective Michael addition of **8** and **9a** (Figure 3), the squaramide catalysts **5**−**7** (Figure 2) have been tested in different solvents and at varying temperatures.

A strong dependence on the solvent, with ee values varying from 41% in diethyl ether to 80% in 1,4-dioxane, is apparent at room temperature (Table 2). Variation of the reaction temperature only slightly influences the selectivity of catalyst **6**[15] in 1,4-dioxane, while the yields rise from 62% at 20 °C to 83% at 5 °C (Table 2, entries 10 and 12).

The influence of the catalyst loading on the reaction was examined by using 5 mol % (Table 2, entry 13) and 20 mol % (Table 2, entry 14) of catalyst **6**.[15] While the yields decrease to 58% for 5 mol % and 74% for 20 mol % catalyst loading, the enantiomeric excess is only slightly altered (Table 2).

The optimized reaction conditions have been applied with catalyst **6**[15] in Michael additions of **8** to different *β*-nitrostyrenes **9**[39,40] (Table 3). Relative to unsubstituted **10a**, lower selectivities, ranging from 53% ee for a chloro substituent in an ortho position (**10d**) to 75% ee for either a methoxy (**10e**) or bromo substituent (**10f**) in a para position of the aromatic compound, are apparent (Table 3).

The yields vary between 42% for the *p*-NMe_2-substituted product **10i** to a maximum of 93% for the *p*-bromo-substituted product **10f** (Table 3). In the case of deactivated aromatic compounds **10g,h**, a different reactivity is observed: The *p*-cyano-substituted product **10h** can only be obtained in traces,

Table 1. Thiourea (1,[9] 2, 3,[10] 4;[11] Figure 1) and Squaramide Catalysts (5, 6,[15] 7;[16] Figure 2) in the Michael Addition of 4-Hydroxycoumarin 8 to *β*-nitrostyrene 9a (Figure 3) at 20 °C

catalyst	time (h:min)	yield (%)	ee (%)
1	6	55	64 (*R*)[a,c]
2	6	60	66 (*R*)[a,c]
3	6	64	48 (*R*)[a,c]
4	6	54	47 (*R*)[a,c]
5	1:30	80	74 (*R*)[b,c]
6	1:30	92	72 (*R*)[b,c]
7	2	70	rac[b,c]

[a]Determined by chiral HPLC analysis ((*R*,*R*)-Whelk O1 column). [b]Determined by chiral HPLC analysis (Chiralcel AD-H column). [c]The *R* configuration is assigned by correlation of computed and experimental optical (−) rotation (Table 4).

Table 2. Solvent Screenings in the Michael Addition of 4-Hydroxycoumarin 8 to *β*-Nitrostyrene 9a Employing Catalysts 5, 6,[15] and 7[16] (Figure 2)

entry	catalyst[a]	solvent	temp (°C)	time (h)	yield (%)	ee[b,c] (%)
1	**5**	1,4-diox	20	1.5	70	72 (*R*)
2	**5**	1,4-diox	10	3	75	77 (*R*)
3	**5**	DCM	20	1.5	67	55 (*R*)
4	**6**	DCM	20	1.5	45	52 (*R*)
5	**6**	1,2-DCE	20	1.5	68	68 (*R*)
6	**6**	$CDCl_3$	20	1.5	90	68 (*R*)
7	**6**	Et_2O	20	4	72	41 (*R*)
8	**6**	MeCN	20	3	70	45 (*R*)
9	**6**	DMSO	20	3	n.d.	rac
10	**6**	1,4-diox	20	1.5	62	80 (*R*)
11	**6**	1,4-diox	10	3	78	81 (*R*)
12	**6**	1,4-diox	5	3	83	79 (*R*)
13	**6**[d]	1,4-diox	10	3	58	79 (*R*)
14	**6**[e]	1,4-diox	10	3	74	80 (*R*)
15	**7**	1,4-diox	10	3	n.d.	5 (*S*)

[a]10 mol % catalyst loading. [b]Determined by chiral HPLC analysis (Chiralcel AD-H column). [c]The *R* configuration is assigned by correlation of computed and experimental optical (−) rotation (Table 4). [d]5 mol % catalyst loading. [e]20 mol % catalyst loading.

DOI: 10.1021/acs.joc.5b02167
J. Org. Chem. 2016, 81, 1762−1768

Table 3. Michael Addition of 4-Hydroxycoumarin 8 to β-Nitrostyrenes 9 Catalyzed by Squaramide 6[15] (Figures 2 and 3)[a]

	styrene				
product	X	Y	Z	yield (%)	ee[b,c] (%)
10a	H	H	H	78	81 (*R*)
10b	H	H	OMe	55	56 (*R*)
10c	H	Br	H	49	58 (*R*)
10d	Cl	H	H	69	53 (*R*)
10e	OMe	H	H	59	75 (*R*)
10f	Br	H	H	93	75 (*R*)
10g	NO_2	H	H	41	61 (*R*)[d,e]
10h	CN	H	H	<5	n.d.[f]
10i	NMe_2	H	H	42	58 (*R*)

[a]Conditions unless stated otherwise: 1,4-dioxane, 10 °C, 10 mol % catalyst loading, 3 h. [b]Determined by chiral HPLC analysis (Chiralcel AD-H column). [c]The *R* configuration is assigned by correlation of computed and experimental optical (−) rotation (Table 4). [d]Isolated as oxime cyclization product **11g** after extended reaction time and heating to 35 °C. [e]Conditions: 1,4-dioxane, 20 °C, 10 mol % catalyst loading, 4 days. [f]Conditions: 1,4-dioxane, 20 °C, 10 mol % catalyst loading, 24 h.

identified by ^{1}H NMR spectroscopy, and is not suitable, due to low solubility, for HPLC chromatography. Product **10g** is only obtained as the product of a cyclization to **11g** (Figure 4), an enantiomeric excess of 61% for the isolated major diastereomer, which is due to the extended reaction time of 24 h and heating to 35 °C.

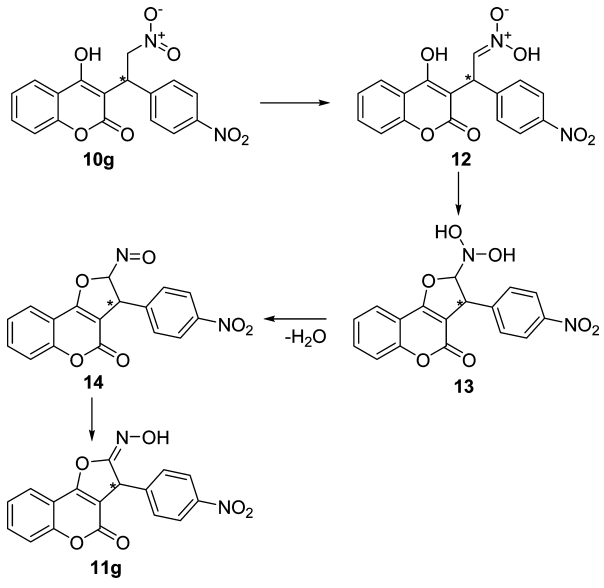

Figure 4. Proposed mechanism for the cyclization of product **10g**.[35]

As shown by Wang et al., the formation of the products **10a**−**i** can be followed by a cyclization procedure[35] (Figure 4). In a first nitro-*aci*-nitro tautomerization **12** is formed, which undergoes cyclization to product **13** (Figure 4). Afterward, **13** is dehydrated to product **14**, which undergoes nitroso−oxime tautomerization, resulting in the experimentally observed oxime **11g** (Figure 4).

To assign the absolute configuration of products **10**, the optical rotation of a scalemic mixture of **10a** (with 77% ee) was measured, resulting in $[\alpha]_D^{20} = -17.6°$ (c = 0.5, EtOAc) for product (−)-**10a** (Table 4). Computations of the optical rotation of conformers of the major product enantiomer, (−)-**10a**, allow the assignment of its absolute configuration of its *R* stereogenic

Table 4. Assignment of the Absolute Configuration of Product (−)-(*R*)-10a

rotamer	ΔA[a] (kcal/mol)	population[b] (%)	comput opt rot[c] (deg)	ϕ comput opt rot (deg)	exp opt rot[d] (deg)
10a-1	0	55.5	−2.3	−154.8	−17.6
10a-2	0.5	23.3	−451.3		
10a-3	0.7	15.9	−146.6		
10a-4	1.4	5.3	−468.4		
10a-5	9.5	≪0.1	−12.4		

[a]Relative free energy at 293.15 K. [b]Boltzmann distribution at 293.15 K.[41−45] [c]Computed optical rotation of different rotamers of product (−)-**10a** (Figure 3) in the gas phase, B3LYP/aug-CC-pVDZ-D3//B3LYP/6-31G*-D3.[41−45,47] [d]Specific optical rotation of **10a** (77% ee, c = 0.5 EtOAc) at 20 °C.

center (Table 4). Different conformers contribute, according to their Boltzmann distribution,[41−45] to a computed average optical rotation of −154.8° for (−)-(*R*)-**10a** (Table 4). Computation of conformers **10a-1** and **10a-5** (Table 4) at a higher level of theory, i.e. B3LYP/aug-CC-pVTZ, results in only slight differences in the optical rotation values: −2.75 and −9.88°, respectively.

DFT computations (B3LYP/6-311++G**D3BJ (1,4-dioxane)//B3LYP/6-31G*) of transition structures with different binding modes explain the selectivity in the Michael addition with catalyst **6**. Binding modes of hydrogen-bonding catalysts proposed by Takemoto[7] (modes A and B, Figure 5) and Pápai[12,46] (modes C and D, Figure 5) are compared for *R* and *S* configurations of **10a**, formed in the Michael addition of **8** to **9a** (Table 5 and Figure 6).

While binding modes A and B show a two-atom binding of the nitro group by the squaramide unit, modes C and D represent a one-atom binding of the enolate by the squaramide scaffold (Figure 5). The most stable transition structure (**TS-1**; Table 5 and Figure 6) yields the *R*-configured **10a**, in agreement with the experiments (Tables 1−3), and exhibits one-atom binding of the enolate of **8** by the squaramide NH groups, while an oxygen atom of the nitro group coordinates the ammonium NH function of the quinuclidine unit of **6**. These squaramide hydrogen-binding distances to the enolate are N_{QN}−H···$O_{coumarin}$ = 1.94 Å and N_{aryl}−H···$O_{coumarin}$ = 1.84 Å (Figure 6 and Table 5). The binding angles of the squaramide unit in **TS-1**, i.e. N_{QN}−H···$O_{coumarin}$ and N_{aryl}−H_{aryl}···$O_{coumarin}$, are 153.9 and 164.0°, respectively (Table 5). The competing, second most stable transition structure **TS-2** (relative energy + 0.1 kcal/mol; Table 5) forms the minor (*S*)-configured product (*S*)-**10a** and shows a one-atom binding mode of one of the nitro oxygen atoms by the squaramide unit (Figure 6), while the enolate coordinates to the ammonium NH function of the quinuclidine unit of **6**. The bond lengths for N_{QN}−H and N_{aryl}−H to O_{nitro} are 1.77 and 1.92 Å, respectively, with binding angles of 159.5 and 163.3°, and the bond length for the quinuclidine unit is N−H···$O_{enolate}$ = 1.83 Å with a binding angle of 154.2° (Table 5).

Four of the five most stable transition structures (**TS1**−**5**) yield the experimentally observed *R* configured product **10a** (Table 3), but the computed energy difference between the most favored **TS1** (*R*) and **TS2** (*S*) is small (0.1 kcal/mol; Table 5 and Figure 6).

The favored one-atom binding mode, as is apparent in the most stable transition structures (**TS1** and **TS2**; Figure 6), is consistent with the canted directionality of its NH units, a frequently encountered structural phenomenon of squaramides.[14]

■ CONCLUSION

An efficient asymmetric Michael addition of 4-hydroxycoumarin **8** to different β-nitrostyrenes **9** is enabled by the bifunctional,

DOI: 10.1021/acs.joc.5b02167
J. Org. Chem. 2016, 81, 1762−1768

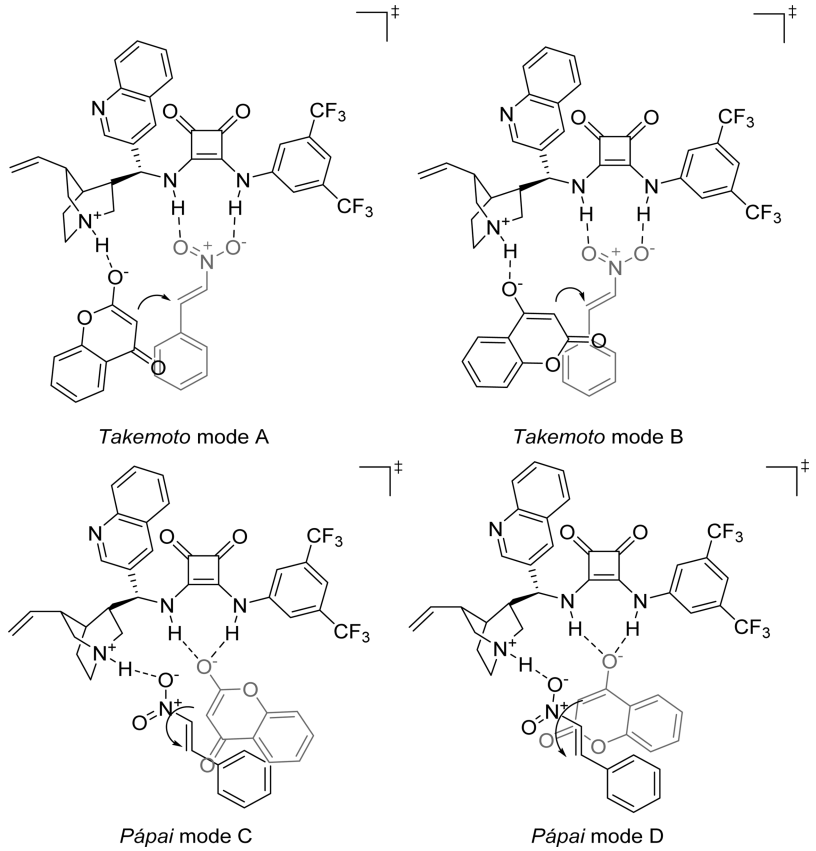

Figure 5. Computed binding modes of transition structures for the Michael addition of 4-hydroxycoumarin **8** to *β*-nitrostyrene **9a** catalyzed by squaramide **6**[15] according to Takemoto[7] and Pápai.[12]

Table 5. Computed Transition Structures for the Michael Addition of 4-Hydroxycoumarin 8 to *β*-Nitrostyrene 9a Catalyzed by Squaramide Catalyst 6[15] **(Figures 5 and 6)**

transition structure (binding mode[a])	total energy (hartree)[b]	ZPE (hartree) (imaginary freq (cm^{-1}))[b,c]	rel energy (kcal/mol)][d]	N_{QN}–H···O (Å/deg)	N_{Ar}–H···O (Å/deg)	formed config
TS-1 (D)	−3175.628052	0.754522 (−293.55)	0.0	1.94/153.9[e]	1.84/164.0[e]	*R*
TS-2 (B)	−3175.628312	0.754941 (−297.36)	0.1	1.77/159.5[f]	1.92/163.3[f]	*S*
TS-3 (C)	−3175.627641	0.754592 (−280.29)	0.3	1.97/153.8[e]	1.81/165.4[e]	*R*
TS-4 (B)	−3175.622063	0.754220 (−257.32)	3.6	1.83/151.4[g]	1.87/154.8[g]	*R*
TS-5 (B)	−3175.621203	0.755002 (−279.81)	4.6	1.87/151.1[f]	2.00/160.6[f]	*R*
TS-6 (B)	−3175.620450	0.754651 (−171.74)	4.9	1.99/150.1[f]	1.89/167.0[f]	*S*
TS-7 (A)	−3175.620392	0.754748 (−277.02)	5.0	1.89/150.5[g]	1.85/152.7[g]	*R*
TS-8 (A)	−3175.620458	0.755075 (−265.09)	5.1	1.91/150.0[f]	1.97/161.3[f]	*R*
TS-9 (B)	−3175.617408	0.754498 (−174.93)	6.7	1.94/152.5[f]	1.92/163.4[f]	*S*
TS-10 (A)	−3175.617331	0.754496 (−167.84)	6.7	2.08/146.5[f]	1.87/166.2[f]	*S*
TS-11 (A)	−3175.616649	0.754530 (−268.58)	7.2	1.79/159.4[f]	1.94/162.6[f]	*S*
TS-12 (B)	−3175.615119	0.754233 (−236.59)	7.9	2.41/135.9[h]	1.81/173.7[h]	*S*
TS-13 (B)	−3175.615649	0.755412 (−317.48)	8.3	1.92/155.9[h]	2.17/141.5[h]	*R*
TS-14 (A)	−3175.610129	0.754250 (−323.55)	11.1	1.85/151.5[f]	1.87/158.5[f]	*S*
TS-15 (B)	−3175.608897	0.754737 (−309.47)	12.2	2.02/132.2[h]	2.11/146.5[h]	*S*
TS-16 (C)	−3175.565809	0.753997 (−288.69)	38.7	1.91/156.6[e]	1.91/163.5[e]	*R*
TS-17 (C)	−3175.560509	0.754667 (−184.33)	42.5	1.99/150.3[f]	1.88/167.2[f]	*S*

[a]Binding mode shown in Figure 5. [b]B3LYP/6-31G* optimized geometries. [c]ZPE, scaled by 0.977.[48] [d]B3LYP/6-311++G**-D3BJ, SCRF (1,4-dioxane)//B3LYP/6-31G*, scaled ZPE corrected. [e]One-atom binding mode to the nucleophile O(coumarin). [f]One-atom binding mode to the electrophile O(nitro). [g]Two-atom binding mode to the electrophile O(nitro). [h]Two-atom binding mode to the nucleophile O(coumarin) and the electrophile O(nitro).

chinchona-derived squaramide catalyst **6**[15] with up to 78% yield and 81% ee (Table 2). This squaramide catalyst proves to be superior to analogue chinchona-derived thiourea catalysts, with respect to reactivity and selectivity. The 3-substituted 4-hydroxycoumarin products **10** all exhibit negative optical rotation ($[\alpha]_D^{20}$) and are assigned as major *R* enantiomers of product **10a**, on the basis of computed optical rotations. Computational analyses of transition structures for the Michael addition of 4-hydroxycoumarin **8** to *β*-nitrostyrene **9a** with chinchona-derived squaramide catalyst **6** show that the most

DOI: 10.1021/acs.joc.5b02167
J. Org. Chem. 2016, 81, 1762−1768

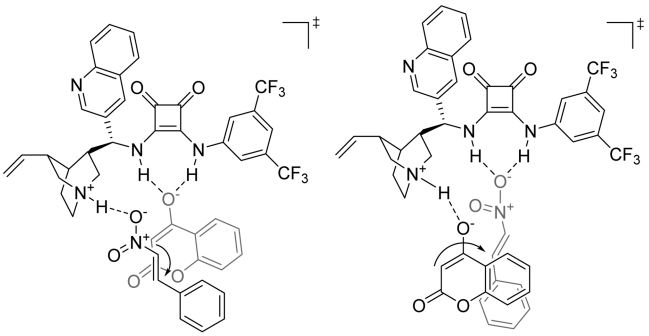

Figure 6. Two competing, most stable transition structures for the Michael addition of 4-hydroxycoumarin **8** to *β*-nitrostyrene **9a** catalyzed by squaramide **6**[15] (B3LYP/6-311++G**-D3BJ, SCRF (1,4-dioxane)//B3LYP/6-31G*; Table S).

stable transition structures, i.e. **TS-1** and **TS2**, exhibit one-atom binding modes of the squaramide unit. While the most stable **TS-1** represents the binding mode D, proposed by Pápai,[12] in **TS-2** (relative energy +0.1 kcal/mol), the binding mode B as proposed by Takemoto[7] is found. Hence, the canted NH functionalities of the squaramide unit in **6** and its favored one-atom binding mode might contribute to the superior performance of catalyst **6** and enable efficient access to pharmacologically relevant 3-substituted 4-hydroxycoumarin products.

EXPERIMENTAL SECTION

Computational Details. In this work the geometry optimizations and frequency computations were performed using GAUSSIAN09[49] at the B3LYP/6-31G(d)[50−55] level of theory. SCRF solvent computations were performed at the B3LYP/6-311++G(d.p)D3BJ[56−59] level of theory. Computations of the optical rotation were performed at the B3LYP/aug-CC-pVDZD3 level of theory.[47,58,59] Zero-point energies were scaled by 0.977.[48]

General Considerations. All reactions were carried out under an argon atmosphere by using Schlenk techniques, unless otherwise stated. Solvents used in chemical conversions were dried by standard methods and distilled under argon prior to use unless otherwise specified. The catalysts **1**−**7** and the *β*-nitrostyrene derivatives **9a**−**i** were prepared according to literature procedures. NMR spectra, HPLC chromatograms, and the coordinates of the computed transition structures and conformers can be found in the Supporting Information.

General Reaction Procedure for the 3-Substituted 4-Hydroxycoumarins. To a stirred solution of 4-hydroxycoumarin (1 equiv) and the corresponding *β*-nitrostyrene (1.2 equiv) in 3 mL of dry 1,4-dioxane at 10 °C was added the organocatalyst (0.1 equiv). The solution was stirred at that temperature for 3 h. After that, the solvent was removed in vacuo and the raw product was purified by flash chromatography. The purified products were analyzed by HPLC chromatography to determine the enantiomeric excess.

*3-(2-Nitro-1-phenyl)ethyl-4-hydroxycoumarin (**10a**).* The reaction was conducted according to the general reaction procedure using 24 mg of 4-hydroxycoumarin (0.15 mmol), 27 mg of *β*-nitrostyrene **9a** (0.18 mmol), and 9.5 mg of catalyst **6** (0.015 mmol). The product was obtained as a white solid after flash chromatography (EtOAc/*n*-Hex 1/1). The analytical data match those in the literature.[25] Yield: 36.4 mg (78%). $[\alpha]_D^{20}$ = −17.6° (*c* = 0.5 EtOAc). ^{1}H NMR (300 MHz, DMSO-d_6): *δ* 8.06 (dd, *J* = 8.2, 1.6 Hz, 1H, H_{Ar}), 7.64 (ddd, *J* = 8.6, 7.3, 1.6, 1H, H_{Ar}), 7.44−7.20 (m, 7H, H_{Ar}), 5.45 (d, *J* = 7.8 Hz, 2H), 5.29 (t, *J* = 7.8 Hz, 1H). ^{13}C{^{1}H} APT NMR (75 MHz, DMSO-d_6): *δ* 162.0, 161.7, 152.2, 138.8, 132.4, 128.4, 127.4, 127.0, 124.0, 123.6, 116.3, 115.8, 104.0, 76.5, 38.4; GC-MS EI (70 eV): t_r(min) = 15.9; calculated $[M - NO_2 - H]^\bullet$ 264.1, found $[M - NO_2 - H]^\bullet$ 264.1. HPLC (Chiralcel AD-H, iPrOH/*n*-hexane 20/80, 1 mL/min, 35 bar): 81% ee, $t_{r,min}$ = 8 min, $t_{r,maj}$ = 10.5 min.

*3-(1-(2-Methoxyphenyl)-2-nitro)ethyl-4-hydroxycoumarin (**10b**).* The reaction was conducted according to the general reaction procedure using 24 mg of 4-hydroxycoumarin (0.15 mmol), 32 mg of *β*-nitrostyrene **9b** (0.18 mmol), and 9.5 mg of catalyst **6** (0.015 mmol). The product was obtained as a white solid after flash chromatography (EtOAc/*n*-Hex 1/1). The analytical data match those in the literature.[25] Yield: 28.2 mg (55%). ^{1}H NMR (300 MHz, DMSO-d_6): *δ* 8.03 (dd, *J* = 8.2, 1.5 Hz, 1H, H_{Ar}), 7.63 (td, *J* = 7.7, 1.5 Hz, 1H, H_{Ar}), 7.45−7.31 (m, 2H, H_{Ar}), 7.32−7.17 (m, 2H, H_{Ar}), 6.99 (dd, *J* = 8.3, 1.1 Hz, 1H, H_{Ar}), 6.88 (td, *J* = 7.5, 1.1 Hz, 1H, H_{Ar}), 5.50 (dd, *J* = 9.0, 6.3 Hz, 1H), 5.37 (dd, *J* = 12.9, 9.0 Hz, 1H), 5.17 (dd, J= 12.9, 6.3 Hz, 1H) 3.79 (s, 3H). ^{13}C{^{1}H} APT NMR (75 MHz, DMSO-d_6): *δ* 162.2, 161.8, 156.7, 152.2, 132.3, 128.3, 128.2, 125.7, 123.5, 123.4, 120.1, 116.3, 115.9, 110.9, 102.7, 75.7, 55.5, 33.6. GC-MS EI (70 eV): t_r(min) = 16.7, calculated $[M - NO_2 - H]^\bullet$ 294.1, found $[M - NO_2 - H]^\bullet$ 294.1. HPLC (Chiralcel AD-H, iPrOH/*n*-hexane 20/80, 1 mL/min, 35 bar): 56% ee, $t_{r,min}$ = 9.4 min, $t_{r,maj}$ = 11.3 min.

*3-(1-(3-Bromophenyl)-2-nitro)ethyl-4-hydroxycoumarin (**10c**).* The reaction was conducted according to the general reaction procedure using 24 mg of 4-hydroxycoumarin (0.15 mmol), 41 mg of *β*-nitrostyrene **9c** (0.18 mmol), and 9.5 mg of catalyst **6** (0.015 mmol). The product was obtained as a white solid after flash chromatography (EtOAc/*n*-Hex 1/1). Yield: 28.7 mg (49%). ^{1}H NMR (300 MHz, DMSO-d_6): *δ* 8.10−8.02 (m, 1H, H_{Ar}), 7.83 (dd, *J* = 7.8, 1.3 Hz, 1H, H_{Ar}), 7.40 (m, 6H, H_{Ar}), 5.44 (t, *J* = 7.4 Hz, 2H), 5.27 (t, *J* = 7.7 Hz, 1H). ^{13}C{^{1}H} APT NMR (75 MHz, DMSO-d_6): *δ* 166.0, 163.0, 162.2, 142.1, 133.1, 131.0, 130.6, 130.4, 127.1, 124.3, 124.1, 123.6, 116.8, 91.4, 76.6, 38.6. GC-MS EI (70 eV): t_r(min) = 16.9, calculated $[M - NO_2 - H]^\bullet$ 343.0, found $[M - NO_2 - H]^\bullet$ 343.9. HRMS (ESI-FTMS): *m*/*z* $[M + Na]^+$ calcd for $C_{17}H_{13}BrNO_5$ 411.9791, found 411.9795. HPLC (Chiralcel AD-H, iPrOH/*n*-hexane 20/80, 1 mL/min, 35 bar): 58% ee, $t_{r,min}$ = 6.8 min, $t_{r,maj}$ = 8.3 min.

*3-(1-(4-Chlorophenyl)-2-nitro)ethyl-4-hydroxycoumarin (**10d**).* The reaction was conducted according to the general reaction procedure using 24 mg of 4-hydroxycoumarin (0.15 mmol), 33 mg of *β*-nitrostyrene **9d** (0.18 mmol), and 9.5 mg of catalyst **6** (0.015 mmol). The product was obtained as a white solid after flash chromatography (EtOAc/*n*-Hex 3/2). The analytical data match those in the literature.[25] Yield: 35.8 mg (69%). ^{1}H NMR (300 MHz, DMSO-d_6): *δ* 8.08−8.02 (m, 1H, H_{Ar}), 7.62 (t, *J* = 7.7 Hz, 1H, H_{Ar}), 7.47−7.32 (m, 6H, H_{Ar}), 5.43 (dd, *J* = 7.7, 3.5 Hz, 2H), 5.28 (t, *J* = 7.7 Hz, 1H). ^{13}C{^{1}H} APT NMR (75 MHz, DMSO-d_6): *δ* 162.5, 161.8, 152.2, 138.0, 132.4, 131.6, 129.4, 128.3, 123.9, 123.7, 123.9, 116.3, 116.0, 103.3, 76.3, 37.9. GC-MS EI (70 eV): t_r(min) = 16.9, calculated $[M - NO_2 - H]^\bullet$ 398.0, found $[M - NO_2 - H]^\bullet$ 398.1. HPLC (Chiralcel AD-H, iPrOH/*n*-hexane 20/80, 1 mL/min, 35 bar): 53% ee, $t_{r,min}$ = 20.7 min, $t_{r,maj}$ = 29.8 min.

*3-(1-(4-Methoxyphenyl)-2-nitro)ethyl-4-hydroxycoumarin (**10e**).* The reaction was conducted according to the general reaction procedure using 24 mg of 4-hydroxycoumarin (0.15 mmol), 32 mg of *β*-nitrostyrene **9e** (0.18 mmol), and 9.5 mg of catalyst **6** (0.015 mmol). The product was obtained as a colorless liquid after flash chromatography (EtOAc/*n*-Hex 3/2). The analytical data match those in the literature.[25] Yield: 30.2 mg (59%). ^{1}H NMR (300 MHz, DMSO-d_6): *δ* 8.03 (dd, *J* = 8.2, 1.6 Hz, 1H, H_{Ar}), 7.63 (ddd, *J* = 8.6, 7.3, 1.1 Hz 1H, H_{Ar}), 7.45−7.23 (m, 4H, H_{Ar}), 6,98−6.76 (m, 2H, H_{Ar}), 5.39 (dd, *J* = 7.9, 2.4 Hz, 2H), 5.21 (t, *J* = 7.9 Hz, 1H). HPLC (Chiralcel AD-H, iPrOH/*n*-hexane 20/80, 1 mL/min, 35 bar): 75% ee, $t_{r,min}$ = 21.5 min, $t_{r,maj}$ = 31.6 min.

*3-(1-(4-Bromophenyl)-2-nitro)ethyl-4-hydroxycoumarin (**10f**).* The reaction was conducted according to the general reaction procedure using 24 mg of 4-hydroxycoumarin (0.15 mmol), 41 mg of *β*-nitrostyrene **9f** (0.18 mmol), and 9.5 mg of catalyst **6** (0.015 mmol). The product was obtained as a pale yellow liquid after flash chromatography (EtOAc/*n*-Hex 3:1). Yield: 54.4 mg (93%). ^{1}H NMR (300 MHz, DMSO-d_6): *δ* 8.04 (dd, *J* = 8.2, 1.5 Hz, 1H, H_{Ar}), 7.62 (ddd, *J* = 8.7, 7.3, 1.5 Hz, 1H, H_{Ar}), 7.50 (d, *J* = 8.5 Hz, 2H, H_{Ar}), 7.37 (m, 4H, H_{Ar}), 5.42 (m, 2H), 5.24 (t, *J* = 7.7 Hz, 1H). ^{13}C{^{1}H} APT NMR (75 MHz, DMSO-d_6): *δ* 163.3, 162.3, 152.8, 139.0, 132.9, 131.7, 130.3,

DOI: 10.1021/acs.joc.5b02167
J. Org. Chem. 2016, 81, 1762−1768

124.4, 124.2, 120.5, 116.8, 116.7, 103.5, 76.7, 38.5. HRMS (ESI-FTMS): m/z $[M + Na]^+$ calcd for $C_{17}H_{13}BrNO_5$ 411.9791, found 411.9794. HPLC (Chiralcel AD-H, iPrOH/*n*-hexane 20/80, 1 mL/min, 35 bar): 75% ee, $t_{r,min}$ = 14.2 min, $t_{r,maj}$ = 20.8 min.

*2-(Hydroxyimino)-3-(4-nitrophenyl)-2,3-dihydro-4H-furo[3,2-c]-chromen-4-one (**10g**).* The reaction was conducted according to the general reaction procedure using 24 mg of 4-hydroxycoumarin (0.15 mmol), 35 mg of *β*-nitrostyrene **9g** (0.18 mmol), and 9.5 mg of catalyst **6** (0.015 mmol). The major diastereomer of the product was obtained as a pale yellow liquid after flash chromatography (EtOAc/*n*-Hex 1/2). Yield: 21.5 mg (41%). ^{1}H NMR (300 MHz, DMSO-d_6): δ 10.72 (s, 1H), 8.19 (d, J = 8.5 Hz, 2H, H_{Ar}), 7.92 (d, J = 7.8 Hz, 1H, H_{Ar}), 7.80 (t, J = 8.0 Hz, 1H, H_{Ar}), 7.68 (d, J = 8.4 Hz, 2H, H_{Ar}), 7.62−7.43 (m, 2H, H_{Ar}), 5.69 (s, 1H). ^{13}C{^{1}H} APT NMR (75 MHz, DMSO-d_6): δ 130.0, 128.1, 124.3, 124.0, 123.9, 117.5, 110.0, 82.1, 81.7, 76.6, 69.5, 41.5, 27.7. HRMS (ESI-FTMS): m/z $[M + H]^+$ calcd for $C_{17}H_{11}N_2O_6$ 339.0611, found 339.06146. HPLC (Chiralcel AD-H, iPrOH/*n*-hexane 20/80, 1 mL/min, 35 bar): 61% ee, $t_{r,maj}$ = 45.2 min, $t_{r,min}$ = 47.6 min.

*3-(1-(4-Cyanophenyl)-2-nitro)ethyl-4-hydroxycoumarin (**10h**).* The reaction was conducted according to the general reaction procedure using 24 mg of 4-hydroxycoumarin (0.15 mmol), 31 mg of *β*-nitrostyrene **9h** (0.18 mmol), and 9.5 mg of catalyst **6** (0.015 mmol). The product was obtained as a pale yellow liquid after flash chromatography (EtOAc/*n*-Hex 2:1). Yield: n.d. (<5%). ^{1}H NMR (300 MHz, DMSO-d_6): δ 7.80 (d, J = 8.2 Hz, 1H, H_{Ar}), 7.68 (d, J = 8.3 Hz, 2H, H_{Ar}), 7.63 (d; J = 8.5 Hz, 2H, H_{Ar}), 7.38−7.33 (m, 1H, H_{Ar}), 7.10 (d, J = 7.5 Hz, 1H, H_{Ar}), 7.05 (d, J = 8.3 Hz, 1H, H_{Ar}), 5.63−5.53 (m, 1H), 5.27−5.16 (m, 2H). HRMS (ESI-FTMS): m/z $[M + Na]^+$ calcd for $C_{18}H_{12}N_2O_5Na$ 359.0638, found 359.0641.

*3-(1-(4-N,N-Dimethylaminophenyl)-2-nitro)ethyl-4-hydroxycoumarin (**10i**).* The reaction was conducted according to the general reaction procedure using 24 mg of 4-hydroxycoumarin (0.15 mmol), 35 mg of *β*-nitrostyrene **9i** (0.18 mmol), and 9.5 mg of catalyst **6** (0.015 mmol). The product was obtained as a pale red solid after flash chromatography (EtOAc/*n*-Hex 1/1). Yield: 21.7 mg (42%). ^{1}H NMR (300 MHz, DMSO-d_6): δ 8.01 (dd, J = 8.3, 1.5 Hz, 1H, H_{Ar}), 7.62 (td, J = 7.9, 7.4, 1.5 Hz, 1H, H_{Ar}), 7.44−7.33 (m, 2H, H_{Ar}), 7.23 (d, J = 8.8 Hz, 2H, H_{Ar}), 6.67 (d, J = 8.8 Hz, 2H, H_{Ar}), 5.37 (dd, J = 8.0, 6.3 hz, 2H), 5.16 (t, J = 7.9 Hz, 1H). ^{13}C{^{1}H} APT NMR (75 MHz, DMSO-d_6): δ 172.3, 164.3, 154.0, 149.4, 132.1, 131.5, 130.0, 128.8, 125.2, 123.6, 122.0, 115.7, 112.7, 97.2, 79.5, 56.5, 56.2, 40.9, 19.0. HRMS (ESI-FTMS): m/z $[M + H^+]^+$ calcd for $C_{19}H_{19}N_2O_5$ 355.1288, found 355.1290; $[M + Na^+]^+$ calcd for $C_{19}H_{18}N_2O_5Na$ 377.1108, found 377.1103. HPLC (Chiralcel AD-H, iPrOH/*n*-hexane 20/80, 1 mL/min, 35 bar): 58% ee, $t_{r,min}$ = 8.9 min, $t_{r,maj}$ = 11.9 min.

■ ASSOCIATED CONTENT

Supporting Information

The Supporting Information is available free of charge on the ACS Publications website at DOI: 10.1021/acs.joc.5b02167.

NMR spectra, HPLC analysis, and coordinates of the computed structures (PDF)

■ AUTHOR INFORMATION

Corresponding Author

*E-mail for B.G.: goldfuss@uni-koeln.de.

Notes

The authors declare no competing financial interest.

■ ACKNOWLEDGMENTS

We thank the Fonds der Chemischen Industrie, the Deutsche Forschungsgemeinschaft, Bayer AG, BASFAG, Wacker AG, Evonic AG, Raschig GmbH, Symrise GmbH, Solvay GmbH, the OMG group, and INEOS- Köln for support. We also thank the computing center of the University of Cologne (RRZK) for providing CPU time on the DFG-funded supercomputer CHEOPS, as well as for support.

■ REFERENCES

(1) Taylor, M. S.; Jacobsen, E. N. *Angew. Chem., Int. Ed.* **2006**, *45*, 1520−1543.
(2) Schreiner, P. R. *Chem. Soc. Rev.* **2003**, *32*, 289−296.
(3) Grondal, C.; Jeanty, M.; Enders, D. *Nat. Chem.* **2010**, *2*, 167−178.
(4) MacMillan, D. W. C. *Nature* **2008**, *455*, 304−308.
(5) Dalko, P. I.; Moisan, L. *Angew. Chem., Int. Ed.* **2004**, *43*, 5138−5175.
(6) Sigman, M. S.; Jacobsen, E. N. *J. Am. Chem. Soc.* **1998**, *120*, 4901−4902.
(7) Okino, T.; Hoashi, Y.; Furukawa, T.; Xu, X.; Takemoto, Y. *J. Am. Chem. Soc.* **2005**, *127*, 119−125.
(8) Zhang, A.; Schreiner, P. R. *Chem. Soc. Rev.* **2009**, *38*, 1187−1189.
(9) Ye, J.; Dixon, D. J.; Hynes, P. S. *Chem. Commun.* **2005**, *2005*, 4481−4483.
(10) Vakulya, B.; Varga, S.; Csámpai, A.; Soós, T. *Org. Lett.* **2005**, *7*, 1967−1969.
(11) Okino, T.; Hoashi, Y.; Takemoto, Y. *J. Am. Chem. Soc.* **2003**, *125*, 12672−12673.
(12) Hamza, A.; Schubert, G.; Soós, T.; Pápai, I. *J. Am. Chem. Soc.* **2006**, *128*, 13151−13160.
(13) Malerich, J. P.; Hagihara, K.; Rawal, V. H. *J. Am. Chem. Soc.* **2008**, *130*, 14416−14417.
(14) Alemán, J.; Parra, A.; Jiang, H.; Jorgensen, K. A. *Chem. - Eur. J.* **2011**, *17*, 6890−6899.
(15) Yang, W.; Du, D.-M. *Org. Lett.* **2010**, *12*, 5450−5453.
(16) Lee, J. W.; Ryu, T. H.; Oh, J. S.; Bae, H. Y.; Jang, H. B.; Song, C. E. *Chem. Commun.* **2009**, 7224−7226.
(17) Storer, R. I.; Aciro, C.; Jones, L. H. *Chem. Soc. Rev.* **2011**, *40*, 2330−2346.
(18) Rotger, C.; Soberats, B.; Quiñonero, D.; Frontera, A.; Ballester, P.; Benet-Buchholz, J.; Deyà, P. M.; Costa, A. *Eur. J. Org. Chem.* **2008**, *2008*, 1864−1868.
(19) Ni, X.; Li, X.; Wang, Z.; Cheng, J.-P. *Org. Lett.* **2014**, *16*, 1786−1789.
(20) Walvoord, R. R.; Huynh, P. N. H.; Kozlowski, M. C. *J. Am. Chem. Soc.* **2014**, *136*, 16055−16065.
(21) Nödling, A. R.; Jakab, G.; Schreiner, P. R.; Hilt, G. *Eur. J. Org. Chem.* **2014**, *2014*, 6394−6398.
(22) Amendola, V.; Bergamaschi, G.; Boiocchi, M.; Fabrizzi, L.; Milani, M. *Chem. - Eur. J.* **2010**, *16*, 4368−4380.
(23) Cranwell, P. B.; Hiscock, J. R.; Haynes, C. J. E.; Light, M. E.; Wells, N. J.; Gale, P. A. *Chem. Commun.* **2013**, *49*, 874−876.
(24) Klare, H.; Hanft, S.; Neudörfl, J. M.; Schlörer, N. E.; Griesbeck, A.; Goldfuss, B. *Chem. - Eur. J.* **2014**, *20*, 11847−11855.
(25) Barange, D. K.; Kavala, V.; Kuo, C.-W.; Lei, P.-M.; Yao, C.-F. *Tetrahedron* **2011**, *67*, 2870−2877.
(26) Chang, X.; Wang, Q.; Wang, Y.; Song, H.; Zhou, Z.; Tang, C. *Eur. J. Org. Chem.* **2013**, *2013*, 2164−2171.
(27) Bye, A.; King, H. K. *Biochem. J.* **1970**, *117*, 237−245.
(28) Yamamoto, Y.; Kurazono, M. *Bioorg. Med. Chem. Lett.* **2007**, *17*, 1626−1628.
(29) O'Reilly, R. A. *N. Engl. J. Med.* **1976**, *295*, 354−357.
(30) Fishelovitch, D.; Hazan, C.; Shaik, S.; Wolfson, H. J.; Nussinov, R. *J. Am. Chem. Soc.* **2007**, *129*, 1602−1611.
(31) Wybranowski, T.; Ziomkowska, B.; Cwynar, A.; Kruzewski, S. *Optica Applicata* **2014**, *XLIV*, 357−364.
(32) Oliphant, C. S.; McCullough, J.; Hashim, T.; Khouzam, R. N. *Future Cardiol.* **2014**, *10*, 229−233.
(33) Shimizu, T.; Takahata, M.; Kameda, Y.; Hamano, H.; Ito, T.; Kimura-Suda, H.; Todoh, M.; Tadano, S.; Iwasaki, N. *Bone* **2014**, *64*, 95−101.
(34) Daly, A. K. *Arch. Toxicol.* **2013**, *87*, 407−420.
(35) Mei, R.-Q.; Xu, X.-Y.; Peng, L.; Wang, F.; Tian, F.; Wang, L.-X. *Org. Biomol. Chem.* **2013**, *11*, 1286−1289.
(36) Leven, M.; Neudörfl, J. M.; Goldfuss, B. *Beilstein J. Org. Chem.* **2013**, *9*, 155−165.
(37) Klare, H.; Neudörfl, J. M.; Goldfuss, B. *Beilstein J. Org. Chem.* **2014**, *10*, 224−236.

DOI: 10.1021/acs.joc.5b02167
J. Org. Chem. 2016, 81, 1762−1768

(38) Rostami, A.; Colin, A.; Li, X. Y.; Chudzinski, M. G.; Lough, A. J.; Taylor, M. S. *J. Org. Chem.* **2010**, *75*, 3983−3992.
(39) McAnda, A. F.; Roberts, K. D.; Smallridge, A. J.; Ten, A.; Trewhella, M. A. *J. Chem. Soc., Perkin Trans. 1* **1998**, *3*, 501−504.
(40) Lopchuk, J. M.; Hughes, R. P.; Gribble, G. W. *Org. Lett.* **2013**, *15*, 5218−5221.
(41) Evidente, A.; Superchi, S.; Cimmino, A.; Mazzeo, G.; Mugnai, L.; Rubiales, D.; Andolfi, A.; Villegas-Fernández, A. M. *Eur. J. Org. Chem.* **2011**, *2011*, 5564−5570.
(42) Karna, S. P.; Dupuis, M. *J. Comput. Chem.* **1991**, *12*, 487−504.
(43) Kondru, R. K.; Wipf, P.; Beratan, D. N. *J. Am. Chem. Soc.* **1998**, *120*, 2204−2205.
(44) Stephens, P. J.; Devlin, F. J.; Cheeseman, J. R.; Frisch, M. J.; Bortolini, O.; Besse, P. *Chirality* **2003**, *15*, 557−564.
(45) Stephens, J. P.; Pan, J. J.; Devlin, F. J.; Cheeseman, J. R. *J. Nat. Prod.* **2008**, *71*, 285−88.
(46) Kótai, B.; Kardos, G.; Hamza, A.; Farkas, V.; Pápai, I.; Soós, T. *Chem. - Eur. J.* **2014**, *20*, 5631−5639.
(47) Dunning, T. H. *J. Chem. Phys.* **1989**, *90*, 1007−1023.
(48) Alecu, I. M.; Zheng, J.; Zhao, Y.; Truhlar, D. G. *J. Chem. Theory Comput.* **2010**, *6*, 2872−2887.
(49) Frisch, M. J.; Trucks, G. W.; Schlegel, H. B.; Scuseria, G. E.; Robb, M. A.; Cheeseman, J. R.; Scalmani, G.; Barone, V.; Mennucci, B.; Petersson, G. A.; Nakatsuji, H.; Caricato, M.; Li, X.; Hratchian, H. P.; Izmaylov, A. F.; Bloino, J.; Zheng, G.; Sonnenberg, J. L.; Hada, M.; Ehara, M.; Toyota, K.; Fukuda, R.; Hasegawa, J.; Ishida, M.; Nakajima, T.; Honda, Y.; Kitao, O.; Nakai, H.; Vreven, T.; Montgomery, J. A., Jr.; Peralta, J. E.; Ogliaro, F.; Bearpark, M.; Heyd, J. J.; Brothers, E.; Kudin, K. N.; Staroverov, V. N.; Keith, T.; Kobayashi, R.; Normand, J.; Raghavachari, K.; Rendell, A.; Burant, J. C.; Iyengar, S. S.; Tomasi, J.; Cossi, M.; Rega, N.; Millam, J. M.; Klene, M.; Knox, J. E.; Cross, J. B.; Bakken, V.; Adamo, C.; Jaramillo, J.; Gomperts, R.; Stratmann, R. E.; Yazyev, O.; Austin, A. J.; Cammi, R.; Pomelli, C.; Ochterski, J. W.; Martin, R. L.; Morokuma, K.; Zakrzewski, V. G.; Voth, G. A.; Salvador, P.; Dannenberg, J. J.; Dapprich, S.; Daniels, A. D.; Farkas, O.; Foresman, J. B.; Ortiz, J. V.; Cioslowski, J.; Fox, D. J. *Gaussian 09, Revision D.01*; Gaussian, Inc., Wallingford, CT, 2013.
(50) Ditchfield, R.; Hehre, W. J.; Pople, J. A. *J. Chem. Phys.* **1971**, *54*, 724−728.
(51) Rassolov, V. A.; Ratner, M. A.; Pople, J. A.; Redfern, P. C.; Curtiss, L. A. *J. Comput. Chem.* **2001**, *22*, 976−984.
(52) Becke, A. D. *J. Chem. Phys.* **1993**, *98*, 5648−5652 (implementation).
(53) Stephens, P. J.; Devlin, F. J.; Chabalowski, C. F.; Frisch, M. J. *J. Phys. Chem.* **1994**, *98*, 11623−11627.
(54) Lee, C.; Yang, W.; Parr, R. G. *Phys. Rev. B: Condens. Matter Mater. Phys.* **1988**, *37*, 785−789.
(55) Miehlich, B.; Savin, A.; Stoll, H.; Preuss, H. *Chem. Phys. Lett.* **1989**, *157*, 200−206.
(56) McLean, A. D.; Chandler, G. S. *J. Chem. Phys.* **1980**, *72*, 5639−5648.
(57) Krishnan, R.; Binkley, J. S.; Seeger, R.; Pople, J. A. *J. Chem. Phys.* **1980**, *72*, 650−654.
(58) Grimme, S.; Antony, J.; Ehrlich, S.; Krieg, H. *J. Chem. Phys.* **2010**, *132*, 154104−1−154104−19.
(59) Grimme, S.; Ehrlich, S.; Goerigk, L. *J. Comput. Chem.* **2011**, *32*, 1456−1465.

DOI: 10.1021/acs.joc.5b02167
J. Org. Chem. 2016, 81, 1762−1768